



PHOTONICS Research

Valence state manipulation of Sm³⁺ ions via a phase-shaped femtosecond laser field

YE ZHENG,¹ YUNHUA YAO,¹ LIANZHONG DENG,^{1,*} WENJING CHENG,² JIANPING LI,¹ TIANQING JIA,¹ JIANRONG QIU,³ ZHENRONG SUN,¹ AND SHIAN ZHANG^{1,4,5}

¹State Key Laboratory of Precision Spectroscopy, East China Normal University, Shanghai 200062, China

²School of Electronic & Electrical Engineering, Shangqiu Normal University, Shangqiu 476000, China

³State Key Laboratory of Silicon Materials, Zhejiang University, Hangzhou 310027, China

⁴Collaborative Innovation Center of Extreme Optics, Shanxi University, Taiyuan 030006, China

⁵e-mail: sazhang@phy.ecnu.edu.cn

*Corresponding author: lzdeng@phy.ecnu.edu.cn

Received 24 October 2017; revised 11 December 2017; accepted 12 December 2017; posted 19 December 2017 (Doc. ID 309766); published 30 January 2018

The ability to manipulate the valence state conversion of rare-earth ions is crucial for their applications in color displays, optoelectronic devices, laser sources, and optical memory. The conventional femtosecond laser pulse has been shown to be a well-established tool for realizing the valence state conversion of rare-earth ions, although the valence state conversion efficiency is relatively low. Here, we first propose a femtosecond laser pulse shaping technique for improving the valence state conversion efficiency of rare-earth ions. Our experimental results demonstrate that the photoreduction efficiency from Sm³⁺ to Sm²⁺ in Sm³⁺-doped sodium aluminoborate glass using a π phase step modulation can be comparable to that using a transform-limited femtosecond laser field, while the peak laser intensity is decreased by about 63%, which is very beneficial for improving the valence state conversion efficiency under the laser-induced damage threshold of the glass sample. Furthermore, we also theoretically develop a (2 + 1) resonance-mediated three-photon absorption model to explain the modulation of the photoreduction efficiency from Sm³⁺ to Sm²⁺ under the π -shaped femtosecond laser field. © 2018 Chinese Laser Press

OCIS codes: (320.5540) Pulse shaping; (320.2250) Femtosecond phenomena; (190.4400) Nonlinear optics, materials; (160.4670) Optical materials.

<https://doi.org/10.1364/PRJ.6.000144>

1. INTRODUCTION

Over the past few decades, the valence state conversion of rare-earth-ion-doped luminescent materials has attracted great attention due to their potential applications in ultrahigh-density 3D optical memories [1,2], broadly tunable lasers [3,4], and so on. In the studies of these rare-earth ions, samarium (Sm) ions were those most studied. For example, Qiu *et al.* observed permanent photoreduction from Sm³⁺ to Sm²⁺ inside a sodium aluminoborate glass irradiated by an infrared (800 nm) femtosecond pulsed laser [5,6], and also demonstrated the recording, readout, and erasure of a 3D optical memory using the valence-state conversion of Sm ions [2]. Jiao *et al.* showed that Sm ions can be selectively incorporated into the precipitated nanophases, which can enhance the photoreduction of Sm³⁺ ions under even lower laser power [7]. Recently, the photoreduction of Sm ions doped in other matrix materials has also aroused considerable interest, such as crystals [8,9], phosphors [10], glass films [11], and glass-ceramics [12,13]. Moreover, the valence state conversion of other rare-earth ions,

like europium (Eu) [14–20] and manganese (Mn) ions [21,22], has also been extensively studied. For example, Lim *et al.* demonstrated that the photoreduction efficiency from Eu³⁺ to Eu²⁺ depends on the initial ion concentration, irradiation laser intensity, and exposure time [16]. Similar phenomena were also observed in the photo-oxidation from Mn²⁺ to Mn³⁺ [22].

Previous studies showed that femtosecond laser pulse excitation provides a very useful strategy for obtaining the valence state conversion of rare-earth ions due to the high laser intensity. In these studies, the researchers usually employed a conventional femtosecond laser pulse with a Gaussian shape, but the valence state conversion efficiency by a Gaussian-shaped femtosecond laser pulse was relatively low. In this work, we first develop a phase-shaped femtosecond laser field to improve the valence state conversion efficiency of rare-earth ions. Our experimental study indicates that the photoreduction efficiency from Sm³⁺ to Sm²⁺ in Sm³⁺-doped sodium aluminoborate glass using a π -shaped femtosecond laser field can be comparable to that using a transform-limited (TL) laser field, but the

peak laser intensity is reduced by about 63%. One important advantage for this experimental observation is that one can obtain a higher photoreduction efficiency of rare-earth ions with a fixed laser intensity under the damage threshold of glass sample. Meanwhile, we also present a (2 + 1) resonance-mediated three-photon absorption model to explain the modulation of photoreduction efficiency from Sm^{3+} to Sm^{2+} using the π -shaped femtosecond laser field, which is very helpful for understanding the physical mechanism of valence state conversion of rare-earth ions in future study.

2. EXPERIMENT ARRANGEMENT

In this study, the glass sample is prepared with a composition in mol ratio of $0.05\text{Sm}_2\text{O}_3 \cdot 10\text{Na}_2\text{O} \cdot 5\text{Al}_2\text{O}_3 \cdot 85\text{B}_2\text{O}_3$. Here, the reagent grade Sm_2O_3 , Na_2CO_3 , Al_2O_3 , and B_2O_3 are used as the starting materials. A mixed 30 g batch is melted in a Pt crucible at 1250°C for 30 min in ambient atmosphere. Then the melt is poured on a stainless steel plate for cooling down. Finally, the synthetic transparent glass sample is polished for optical measurement.

Our experimental arrangement is shown in Fig. 1. The excitation source is a Ti:sapphire mode-locked regenerative amplifier (Spectra-Physics Spitfire) with a pulse width of about 50 fs, a central wavelength of 800 nm, and a repetition rate of 1 kHz. The femtosecond laser spectral phase in the frequency domain is modulated by a programmable $4-f$ configuration zero-dispersion pulse shaper, which is composed of a pair of diffraction gratings of 1200 lines/mm, a pair of concave mirrors with a 200 mm focal length, and a one-dimensional liquid crystal spatial light modulator (SLM; Jenoptik SLM-S320D). The SLM is placed at the Fourier plane and used to control the spectral phase and/or amplitude. The phase-shaped femtosecond laser pulse is focused into the Sm^{3+} -doped sodium aluminoborate glass via a lens with a 10 mm focal length; here the glass sample is fixed on an XYZ stage for fine adjustment. The laser intensity at the focus is estimated to be $\sim 1.3 \times 10^{13} \text{ W/cm}^2$. A continuous wave (CW) laser with a wavelength of 532 nm is used to excite the glass sample after irradiation with an 800 nm femtosecond laser. All the luminescence signals from the glass sample induced

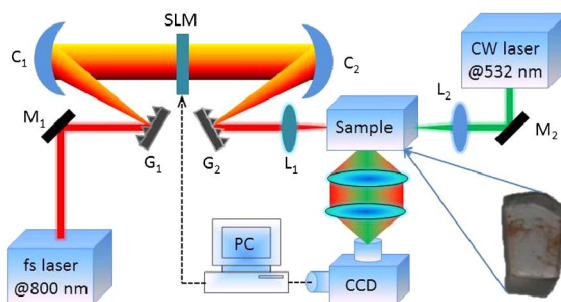


Fig. 1. Experimental arrangement for valence state manipulation in Sm^{3+} -doped sodium aluminoborate glass using a femtosecond laser pulse shaping method. C_1 and C_2 stand for two cylindrical mirrors, M_1 and M_2 are two circular mirrors, G_1 and G_2 are two gratings, and L_1 and L_2 are two focusing lenses. Here, a continuous wave (CW) laser with a wavelength of 532 nm is used to detect the valence state change of Sm^{3+} ions. The inset shows a picture of the glass sample after the femtosecond laser irradiation.

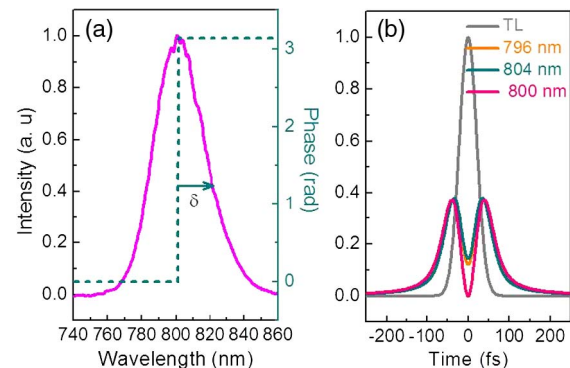


Fig. 2. (a) Femtosecond laser spectrum using π phase step modulation (dark cyan dashed line) and (b) the shaped femtosecond laser pulse shapes with π phase step positions of 796 (orange line), 800 (pink line), and 804 nm (dark cyan line), together with the transform-limited (TL) laser pulse (gray line).

by the 532 nm CW laser are perpendicularly collected by a telescope system, and the corresponding luminescence spectrum is recorded via a spectrometer with a charge-coupled device (CCD).

In this work, we use a π phase step modulation to control the photoreduction efficiency from Sm^{3+} to Sm^{2+} in the Sm^{3+} -doped sodium aluminoborate glass. The π phase step modulation, as a typical phase inversion, has been proven to be a good strategy for the control of various nonlinear optical processes [23]. Figure 2(a) shows this simple phase modulation on the femtosecond laser spectrum. In mathematics, the π phase step modulation can be defined by the function $\varphi(\omega) = \pi\sigma(\omega - \omega_{\text{step}})/2$, where $\sigma(\omega - \omega_{\text{step}})$ denotes the signum function, which takes the values of -1 for $\omega < \omega_{\text{step}}$ and $+1$ for $\omega > \omega_{\text{step}}$. Thus, $\varphi(\omega)$ is characterized by a phase jump from $-\pi/2$ to $\pi/2$ at the step position ω_{step} . The modulated femtosecond laser field in frequency domain $E_{\text{mod}}(\omega)$ can be expressed as $E_{\text{mod}}(\omega) = E(\omega) \times \exp[i\pi\sigma(\omega - \omega_{\text{step}})/2]$, where $E(\omega)$ is the Fourier transform of the unmodulated laser field $E(t)$. The modulated femtosecond laser field in time domain $E_{\text{mod}}(t)$ is given by the convolution of $E(t)$ with $\exp(i\omega_{\text{step}}t)/\pi t$, i.e., $E_{\text{mod}}(t) = E(t) \otimes \exp(i\omega_{\text{step}}t)/\pi t$. Figure 2(b) shows the temporal intensity distribution of the shaped femtosecond laser pulse with the π phase step positions of 796, 800, and 804 nm, together with the TL femtosecond laser pulse. One can see that the π phase step modulation will induce the femtosecond laser pulse splitting and form a double subpulse structure. Thus, the peak laser intensity will be effectively suppressed, and the maximal suppression efficiency can be up to $\sim 63\%$.

3. RESULTS AND DISCUSSION

To observe the valence state conversion of Sm^{3+} -doped sodium aluminoborate glass under irradiation of an 800 nm femtosecond laser pulse, we present the luminescence spectra before and after the femtosecond laser irradiation, as shown in Fig. 3(a). Before the femtosecond laser irradiation, there are three main luminescence peaks around 563, 598, and 645 nm, which can be attributed to the transition processes of Sm^{3+} ions: ${}^4\text{G}_{5/2} \rightarrow {}^6\text{H}_{5/2}$,

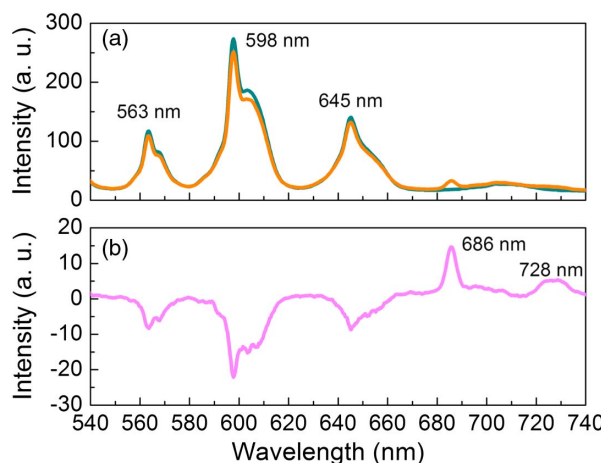


Fig. 3. (a) Luminescence spectra before (dark cyan line) and after (orange line) the shaped femtosecond laser irradiation and (b) the difference between the two luminescence spectra.

${}^4G_{5/2} \rightarrow {}^6H_{7/2}$, and ${}^4G_{5/2} \rightarrow {}^6H_{9/2}$ [24]. After the femtosecond laser irradiation, two new weak luminescence peaks appear around 686 and 728 nm, which are conventionally attributed to the $4f \rightarrow 4f$ transition of Sm^{2+} ions [6]. For better viewing, the difference between the two luminescence spectra is calculated, as shown in Fig. 3(b). As can be seen, the luminescence intensities around 563, 598, and 645 nm decrease, while the luminescence intensities around 686 and 728 nm increase. This experimental observation indicates that a portion of Sm^{3+} ions are converted to Sm^{2+} ions after the femtosecond laser irradiation.

For further verification of the valence state conversion from Sm^{3+} to Sm^{2+} , we also measure the absorption spectra of the glass sample before and after the femtosecond laser irradiation, as shown in Fig. 4(a). Similarly, the difference between the two absorption spectra is also calculated for the convenience of viewing, and the calculated result is plotted in Fig. 4(b). After the femtosecond laser irradiation, two absorption bands can be observed around 210 and 320 nm. The strong absorption band around 210 nm can be ascribed to the charge transfer state and $4f \rightarrow 4f$ transition of Sm^{3+} ions, whereas the weak

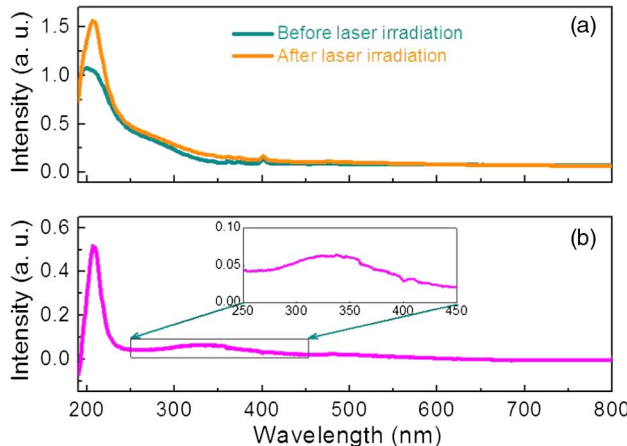


Fig. 4. (a) Absorption spectra of the glass sample before and after the femtosecond laser irradiation and (b) the difference between the two absorption spectra.

absorption band around 320 nm can be mainly ascribed to the $5d \rightarrow 4f$ transition of Sm^{2+} ions [6]. Moreover, we also provide a picture of the glass sample after the femtosecond laser irradiation, as shown in the inset of Fig. 1. The glass sample is colorless before the femtosecond laser irradiation, while it becomes brown after the laser irradiation, which is due to the presence of Sm^{2+} ions.

Obviously, the 800 nm femtosecond laser can provide a well-established tool for realizing the valence state conversion from Sm^{3+} to Sm^{2+} . Next, we study the effect of π phase step modulation on the photoreduction efficiency. For convenience, we only present the two representative luminescence intensities around 600 and 686 nm with an increasing number of laser shots; the experimental results are shown in Fig. 5. Here, we consider the six π phase step positions 750, 790, 796, 800, 804, and 810 nm. When the laser shot number increases, the luminescence intensity around 686 nm shows an evolution process that rapidly decreases and then remains stable. However, the luminescence intensity around 600 nm shows the opposite evolution behavior, a process of rapidly increasing and then approaching stability. It can be seen that the π phase step modulation can effectively control the luminescence intensities of both Sm^{3+} and Sm^{2+} ions, while the control efficiency can only be reduced, but not improved. It is worth noting that the luminescence intensity variation at a wavelength of 686 nm is smaller than that at a wavelength of 600 nm. This difference may be due to the different excitation processes and luminescence efficiencies in Sm^{3+} and Sm^{2+} ions.

As shown in Fig. 5, it is interesting that the luminescence intensity of Sm^{2+} ions at a π phase step position of 800 nm can be comparable to that using the TL femtosecond laser field (also see the case of the π phase step position at 750 nm), but the peak laser intensity under this phase modulation will be greatly suppressed, and is about 37% of the TL laser field. That is, the shaped femtosecond laser field with the lower peak laser intensity can obtain almost the same photoreduction efficiency as the TL femtosecond laser field with the higher peak laser intensity, which is very useful for obtaining the maximum

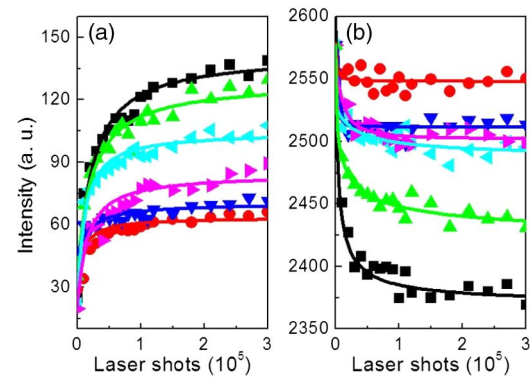


Fig. 5. Luminescence intensities at a wavelength of (a) 686 and (b) 600 nm with an increasing laser shot number for π phase step positions of 750 (black squares), 790 (red circles), 796 (cyan left-pointing triangles), 800 (green upward-pointing triangles), 804 (magenta right-pointing triangles), and 810 nm (blue downward-pointing triangles). Here, the experimental data in (a) and (b) are fitted by the exponential and sigmoidal functions, respectively.

photoreduction efficiency under the laser-induced damage threshold of the glass sample. To demonstrate this, we measure the luminescence intensities at a wavelength of 686 nm with an increasing laser shot number for the π phase step positions of 750 and 800 nm under the same peak laser intensity of $1.3 \times 10^{13} \text{ W/cm}^2$; the experimental results are shown in Fig. 6. As expected, the luminescence intensity using π phase step modulation can be greatly improved, by a factor of ~ 3.6 .

Moreover, an important observation in Fig. 5 is that all the luminescence intensities at the different π phase step positions will reach saturation with an increasing laser shot number; that is, the photoreduction efficiency from Sm^{3+} to Sm^{2+} will be fixed when the laser shot number reaches a certain value (about 2×10^5 for our experiment). This experimental phenomenon can be explained as follows. Under the femtosecond laser excitation, the Sm^{3+} ions can be converted into Sm^{2+} ions by photoreduction, and the Sm^{2+} ions can also be changed back to Sm^{3+} ions by photo-oxidation. At the beginning, the photoreduction from Sm^{3+} to Sm^{2+} dominates the whole process, and the luminescence intensity of Sm^{3+} ions will decrease, while the luminescence intensity of Sm^{2+} ions will increase. With an increasing laser shot number, the number of Sm^{2+} ions will also increase, and the contribution of photo-oxidation from Sm^{2+} to Sm^{3+} will gradually strengthen. Finally, photoreduction and photo-oxidation achieve the balance, and thus the luminescence intensities of both Sm^{3+} and Sm^{2+} ions will approach stability.

To understand the physical control mechanism of valence state conversion from Sm^{3+} to Sm^{2+} with π phase step modulation, we theoretically propose a $(2 + 1)$ resonance-mediated three-photon absorption model to explain the luminescence intensity control of Sm^{2+} ions in Fig. 5(a). Figure 7(a) shows the schematic of the electron–hole generation in the glass sample by the $(2 + 1)$ resonance-mediated three-photon absorption in Sm^{3+} ions. Here, ${}^6\text{H}_{5/2}$ (or valence band) and ${}^6\text{P}_{3/2}$ represent, respectively, the ground state $|g\rangle$ and the intermediate excited state $|i\rangle$, and the conduction band is used as the final excited state $|f\rangle$. The initial population in the ground state ${}^6\text{H}_{5/2}$ is pumped to the excited state ${}^6\text{P}_{3/2}$ by simultaneously absorbing two photons, and then is further excited to the conduction

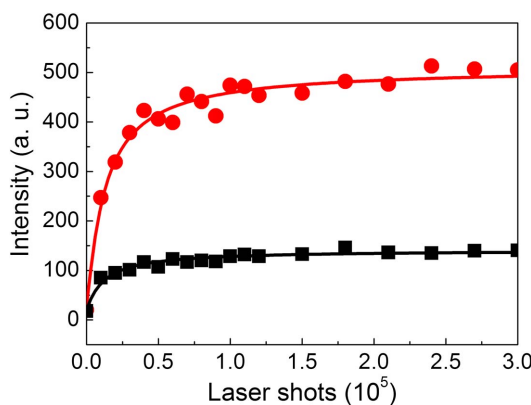


Fig. 6. Luminescence intensities at a wavelength of 686 nm with an increasing laser shot number for π phase step positions of 750 (black squares) and 800 nm (red circles) under the same peak laser intensity of $1.3 \times 10^{13} \text{ W/cm}^2$.

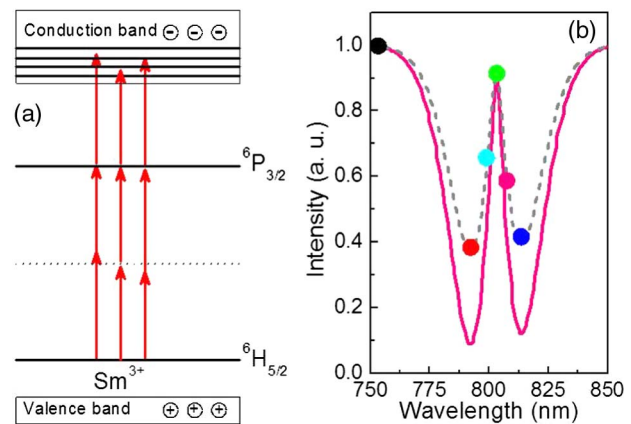


Fig. 7. (a) Schematic of electron–hole generation in the glass sample by a $(2 + 1)$ resonance-mediated three-photon absorption in Sm^{3+} ions, (b) the theoretical calculation of three-photon transition probability by π phase step modulation, together with the corresponding luminescence intensity modulation shown in Fig. 5(a) (circles).

band by absorbing the other photon, which results in the generation of electron–hole pairs in the glass sample. The holes are trapped by nonbridging oxygen ions as well as by tetrahedral capping born atoms, while the electrons are trapped by the Sm^{3+} ions [6]. Thus, the valence state conversion efficiency of Sm^{3+} ions depends on the $(2 + 1)$ resonance-mediated three-photon transition probability.

In the perturbative regime, the $(2 + 1)$ resonance-mediated three-photon transition probability can be approximated by the time-dependent perturbation theory as [25]

$$P^{(2+1)} \propto \int_{-\infty}^{+\infty} d\omega_f A(\omega_f) |A^{(2+1)(\text{on-res})} + A^{(2+1)(\text{near-res})}|^2, \quad (1)$$

where $A^{(2+1)(\text{on-res})}$ and $A^{(2+1)(\text{near-res})}$ represent, respectively, the on- and near-resonant three-photon absorption, and are given by

$$A^{(2+1)(\text{on-res})} \propto i\pi \int_{-\infty}^{+\infty} d\omega_i A(\omega_i) A^{(2)}(\omega_i) E(\omega_f - \omega_i) \quad (2)$$

and

$$A^{(2+1)(\text{near-res})} \propto -i\wp \int_{-\infty}^{+\infty} d\Delta \frac{1}{\Delta} A^{(2)}(\omega_i - \Delta) E(\omega_f - \omega_i + \Delta), \quad (3)$$

with

$$A^{(2)}(\Omega) = \int_{-\infty}^{+\infty} d\omega E(\omega) E(\Omega - \omega), \quad (4)$$

where $A(\omega_i)$ and $A(\omega_f)$ are the absorption line-shape functions of the two excited states $|i\rangle$ and $|f\rangle$, and \wp is Cauchy's principal value. Obviously, the on-resonant term $A^{(2+1)(\text{on-res})}$ in Eq. (2) is the interference of all on-resonant three-photon excitation pathways (i.e., $\Delta = 0$), while the near-resonant term $A^{(2+1)(\text{near-res})}$ in Eq. (3) represents the interference of other non-resonant three-photon excitation pathways (i.e., $\Delta \neq 0$) by the weighting factor $1/\Delta$.

Figure 7(b) shows the calculated results of the $(2 + 1)$ resonance-mediated three-photon transition probability $P^{(2+1)}$

as a function of the π phase step position in the laser wavelength. To facilitate comparison, the normalized luminescence intensities of Sm^{2+} ions in Fig. 5(a) are also given. It is obvious that the control behaviors for the absorption probability of Sm^{3+} ions and the luminescence intensity of Sm^{2+} ions under π phase step modulation are the same, which means that the valence state conversion from Sm^{3+} to Sm^{2+} should result from the electron-hole generation in the Sm^{3+} ions by the (2 + 1) resonance-mediated three-photon absorption. However, it is noted that the control efficiencies of numerical calculation and experimental measurement are different. The discrepancy can be attributed to the different excitation processes or luminescence efficiencies for Sm^{3+} and Sm^{2+} ions. Furthermore, under the intermediate femtosecond laser field, in addition to (2 + 1) resonance-mediated three-photon absorption, there may be other, higher nonlinear optical effects in the excitation process of Sm^{3+} ions, such as five-photon absorption or stimulated Raman scattering.

4. CONCLUSIONS

In summary, we have experimentally observed the valence state conversion from Sm^{3+} to Sm^{2+} in Sm^{3+} -doped sodium aluminoborate glass under the irradiation of the shaped femtosecond laser field with π phase step modulation. Our experimental study indicated that π phase step modulation can effectively control the photoreduction efficiency from Sm^{3+} to Sm^{2+} . Importantly, the shaped femtosecond laser field with the lower laser intensity can obtain almost the same photoreduction efficiency as the unshaped (i.e., TL) femtosecond laser field. Furthermore, a (2 + 1) resonance-mediated three-photon absorption model was proposed to explain the physical control mechanism of photoreduction efficiency modulation from Sm^{3+} to Sm^{2+} under the π -shaped femtosecond laser field. This study provides a feasible method for obtaining higher photoreduction efficiency of rare-earth ions under the laser-induced damage threshold of the glass sample, and also presents clear physical insight into the valence state conversion of rare-earth ions. In addition, the experimental and theoretical results are very helpful for understanding and controlling the valence state conversion of rare-earth ions in future study.

Funding. National Natural Science Foundation of China (NSFC) (11474096, 11727810, 11774094, 61720106009); Science and Technology Commission of Shanghai Municipality (STCSM), China (16520721200, 17ZR146900).

REFERENCES

- D. A. Parthenopoulos and P. M. Rentxepis, "Three-dimensional optical storage memory," *Science* **245**, 843–845 (1989).
- K. Miura, J. Qiu, S. Fujiwara, S. Sakaguchi, and K. Hirao, "Three-dimensional optical memory with rewritable and ultrahigh density using the valence-state change of samarium ions," *Appl. Phys. Lett.* **80**, 2263–2265 (2002).
- G. Baldacchini, M. Cremona, G. d'Auria, R. M. Montereali, and V. Kalinov, "Radiative and nonradiative processes in the optical cycle of the F^3+ center in LiF ," *Phys. Rev. B* **54**, 17508–17514 (1996).
- H. Gu, L. Qi, and L. Wan, "Broadly tunable yellow-green laser using color centers in a LiF crystal at room temperature," *Appl. Phys. Lett.* **52**, 1845–1846 (1988).
- J. Qiu, K. Miura, T. Suzuki, T. Mitsuyu, and K. Hirao, "Permanent photoreduction of Sm^{3+} to Sm^{2+} inside a sodium aluminoborate glass by an infrared femtosecond pulsed laser," *Appl. Phys. Lett.* **74**, 10–12 (1999).
- J. Qiu, K. Miura, K. Nouchi, T. Suzuki, Y. Kondo, T. Mitsuyu, and K. Hirao, "Valence manipulation by lasers of samarium ion in micrometer-scale dimensions inside transparent glass," *Solid State Commun.* **113**, 341–344 (1999).
- Q. Jiao, Z. Song, Z. Yang, X. Yu, and J. Qiu, "Sm³⁺ photoreduction in BaCl_2 nanophases precipitated fluoroaluminate glasses under femtosecond laser irradiation," *Opt. Lett.* **36**, 3091–3093 (2011).
- R. Jaaniso and H. Bill, "Room temperature persistent spectral hole burning in Sm-doped $\text{SrFC}_{1/2}\text{Br}_{1/2}$ mixed crystals," *Europhys. Lett.* **16**, 569–574 (1991).
- M. C. Wiegand, W. Sievers, J. K. N. Lindner, T. Tröster, and S. Schweizer, "Photoluminescence properties of Sm^{2+} -doped BaBr_2 under hydrostatic pressure," *J. Lumin.* **131**, 2400–2403 (2011).
- W. Chen and M. Su, "Stimulated luminescence and photo-gated hole burning in $\text{BaCl}_{0.8}\text{Br}_{0.2}\text{:Sm}^{2+}$, Sm^{3+} phosphors," *J. Phys. Chem. Solids* **60**, 371–378 (1999).
- S. Park, Y. Chung, W. Qin, H. Cho, E. Cho, K. Jang, S. Kim, Y. Lee, and C. Kim, "The influence of metal aluminium on the reduction of the Sm^{3+} doped in aluminosilicate glass films," *J. Phys. Condens. Matter* **16**, 2543–2550 (2004).
- A. Edgar, C. R. Varoy, C. Koughia, D. Tonchev, G. Belev, G. Okada, S. O. Kasap, H. von Seggern, and M. Ryan, "Optical properties of divalent samarium-doped fluorochlorozirconate glasses and glass ceramics," *Opt. Mater.* **31**, 1459–1466 (2009).
- D. Wei, B. Yuan, Y. Huang, T. Tsubio, and H. J. Seo, "Influence of crystallization on the conversion of $\text{Sm}^{3+} \rightarrow \text{Sm}^{2+}$ in $\text{SrO}\text{-}\text{Bi}_2\text{O}_3\text{-K}_2\text{O}\text{-}\text{B}_2\text{O}_3$ glass-ceramics," *J. Am. Ceram. Soc.* **96**, 2167–2171 (2013).
- J. Qiu, Y. Shimizugawa, Y. Iwabuchi, and K. Hirao, "Photostimulated luminescence in Eu^{2+} -doped fluoroaluminate glasses," *Appl. Phys. Lett.* **71**, 759–761 (1997).
- J. Qiu, K. Kojima, K. Miura, T. Mitsuyu, and K. Hirao, "Infrared femtosecond laser pulse-induced permanent reduction of Eu^{3+} to Eu^{2+} in a fluorozirconate glass," *Opt. Lett.* **24**, 786–788 (1999).
- K. S. Lim, S. Lee, M. T. Trinh, S. H. Kim, M. Lee, D. S. Hamilton, and G. N. Gibson, "Femtosecond laser-induced reduction in Eu-doped sodium borate glasses," *J. Lumin.* **122**, 14–16 (2007).
- M. Peng and G. Hong, "Reduction from Eu^{3+} to Eu^{2+} in BaAl_2O_4 : Eu phosphor prepared in an oxidizing atmosphere and luminescent properties of BaAl_2O_4 : Eu," *J. Lumin.* **127**, 735–740 (2007).
- E. Malchukova and B. Boizot, "Reduction of Eu^{3+} to Eu^{2+} in aluminoborosilicate glasses under ionizing radiation," *Mater. Res. Bull.* **45**, 1299–1303 (2010).
- J. A. Sampaio, M. C. Filadelpho, A. A. Andrade, J. H. Rohling, A. N. Medina, A. C. Bento, L. M. daSilva, F. C. G. Gandra, L. A. O. Nunes, and M. L. Baesso, "Study on the observation of Eu^{2+} and Eu^{3+} valence states in low silica calcium aluminosilicate glasses," *J. Phys. Condens. Matter* **22**, 055601 (2010).
- K. Biswas, A. D. Sontakke, R. Sen, and K. Annapurna, "Luminescence properties of dual valence Eu doped nano-crystalline BaF_2 embedded glass-ceramics and observation of $\text{Eu}^{2+} \rightarrow \text{Eu}^{3+}$ energy transfer," *J. Fluoresc.* **22**, 745–752 (2012).
- J. Qiu, C. Zhu, T. Nakaya, J. Si, K. Kojima, F. Ogura, and K. Hirao, "Space-selective valence state manipulation of transition metal ions inside glasses by a femtosecond laser," *Appl. Phys. Lett.* **79**, 3567–3569 (2001).
- S. Lee, M. T. Trinh, J. R. Nam, K. S. Lim, M. Lee, and E. Kim, "Laser-induced defect centers and valence state change of Mn ions in sodium borate glasses," *J. Lumin.* **122**, 142–145 (2007).
- D. Goswami, "Optical pulse shaping approaches to coherent control," *Phys. Rep.* **374**, 385–481 (2003).
- Y. Zheng, W. Cheng, Y. Yao, C. Xu, D. Feng, T. Jia, J. Qiu, Z. Sun, and S. Zhang, "Observation of up-conversion luminescence polarization control in Sm^{3+} -doped glass under an intermediate femtosecond laser field," *RSC Adv.* **7**, 13444–13450 (2017).
- S. Zhang, H. Zhang, T. Jia, Z. Wang, and Z. Sun, "Coherent phase control of (2+1) resonantly enhanced multiphoton ionization photo-electron spectroscopy," *J. Phys. B* **43**, 135401 (2010).